Neuron, Volume *111*

Supplemental information

In vivo photopharmacology with light-activated opioid drugs

Shannan P. McClain, Xiang Ma, Desiree A. Johnson, Caroline A. Johnson, Aryanna E. Layden, Jean C. Yung, Susan T. Lubejko, Giulia Livrizzi, X. Jenny He, Jingjing Zhou, Janie Chang-Weinberg, Emilya Ventriglia, Arianna Rizzo, Marjorie Levinstein, Juan L. Gomez, Jordi Bonaventura, Michael Michaelides, and Matthew R. Banghart

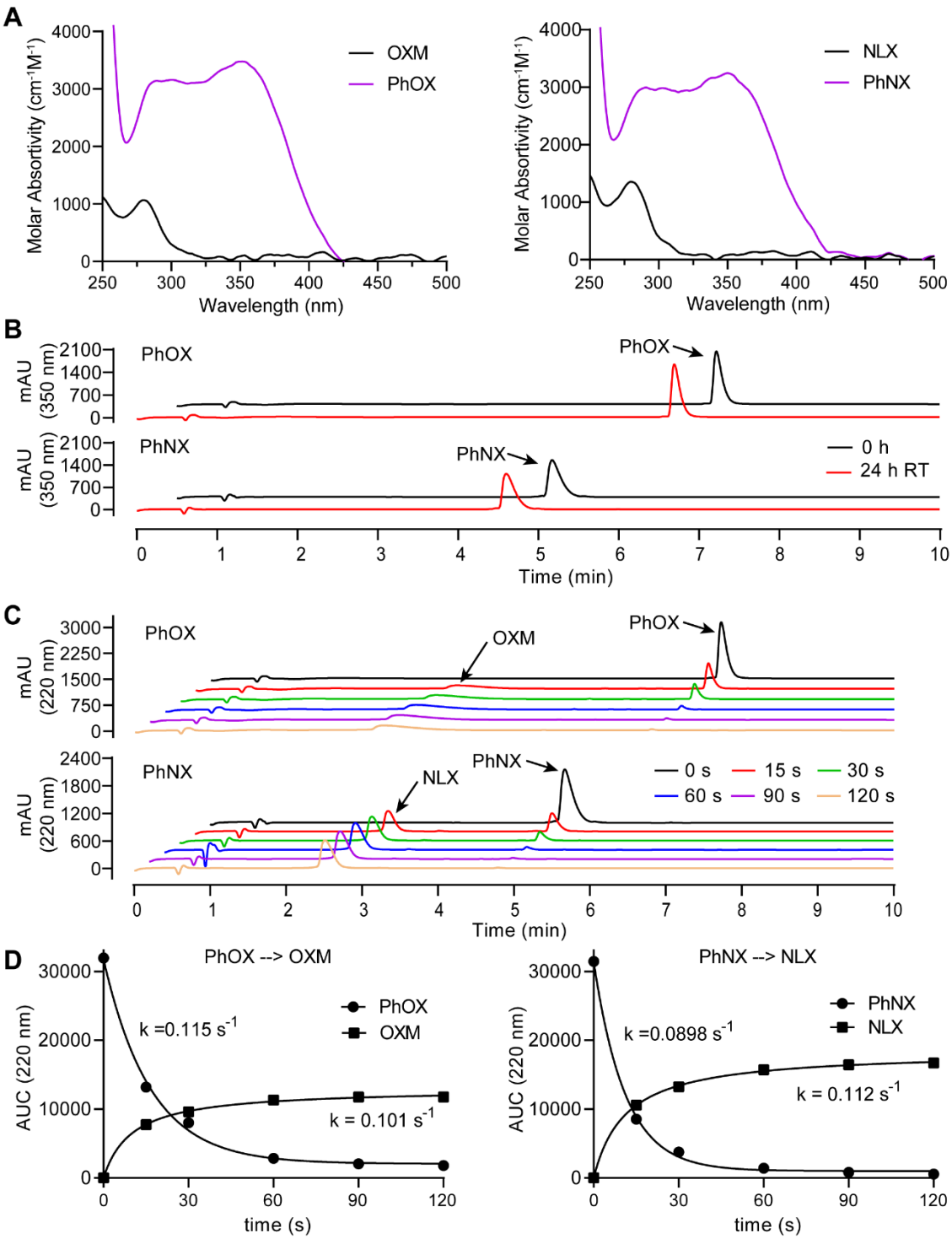

Figure S1. *In vitro* characterization of PhOX and PhNX stability and photolysis, Related to Figure 1. (A) UV/VIS absorbance spectra of PhOX and OXM (left), and PhNX and NLX (right). The DMNPE caging group exhibits minimal absorbance beyond 425 nm, rendering it compatible with fluorescence imaging with visible light-excited fluorophores. **(B)** High

pressure liquid chromatography (HPLC) chromatograms (350 nm absorbance) of samples of PhOX (top) and PhNX (bottom) (1 mM) dissolved in PBS buffer (pH 7.2) before and after being left in the dark at room temperature for 24 hours. The lack of change in the chromatograms indicates that both compounds are highly stable in the absence of illumination. **(C)** Waterfall plots of the HPLC chromatograms (220 nm absorbance) for samples of PhOX (top) and PhNX (bottom) (1 mM) dissolved in PBS buffer (pH 7.2) after being illuminated with 375 nm light for the indicated time periods. **(D)** Summary of PhOX (left) and PhNX (right) photouncaging reactions over time, as measured by HPLC (220 nm absorbance). The area under the curve (AUC) data include the examples shown in Supporting Figure 1C (n=3 samples per compound). The rate constants of starting material loss and product formation were obtained by fitting the curves with a single exponential function. All data are plotted as mean ± SEM.

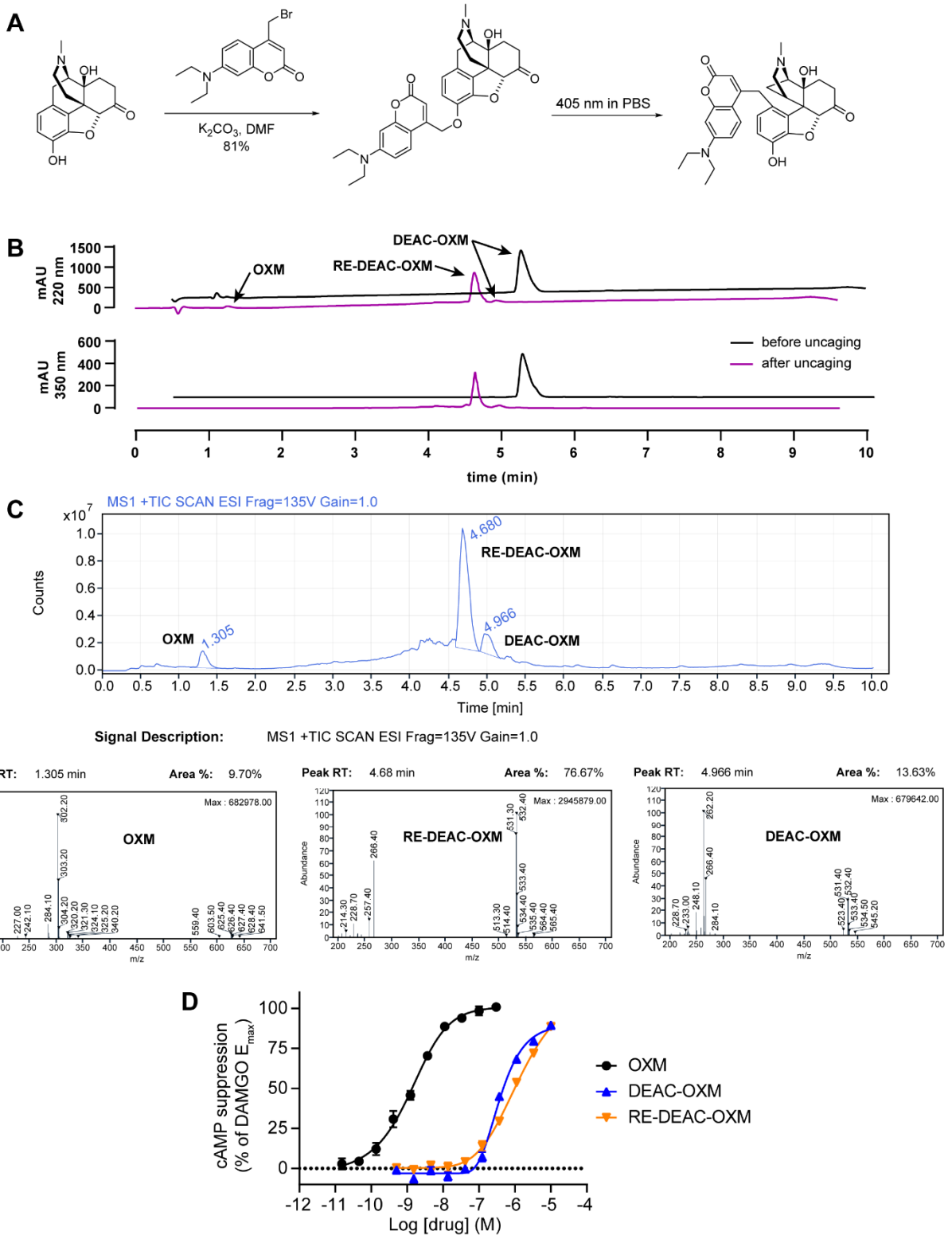

Figure S2. Synthesis and in vitro evaluation of DEAC-OXM, Related to Figure 1. (A) Reaction scheme depicting the one-step alkylation procedure used to synthesize DEAC-OXM

from commercially available oxymorphone (**2**) and DEAC-Br, as well as its photochemical conversion to the proposed primary reaction product "rearranged DEAC-OXM" (RE-DEAC-OXM), which likely occurs via a 1,4-Photo-Claisen rearrangement. **(B)** High pressure liquid chromatography (HPLC) chromatograms measured at 220 nm indicating predominant photoconversion of DEAC-OXM to RE-DEAC-OXM, which has a similar retention time, along with a much smaller amount of OXM in PBS (pH 7.2). **(C)** (Top) LC-MS (mass spectrometry) chromatogram of the reaction mixture shown in B. (Bottom) MS traces revealing that RE-DEAC-OXM has the same molecular weight as DEAC-OXM (531 Da). **(D)** Agonist dose-response curves at the MOR for DEAC-OXM, RE-DEAC-OXM, and OXM using the GloSensor™ assay of cAMP signaling in HEK293T cells. The solid line depicts the best-fit sigmoidal function used to derive the indicated EC_{50} value. OXM EC_{50} = 1.3 nM, DEAC-OXM EC_{50} = 380 nM, RE-DEAC-OXM EC_{50} = 1.3 μM. Data were normalized to the response produced by DAMGO (1 μM) and are expressed as mean ± SEM (n=5-10 wells per concentration).

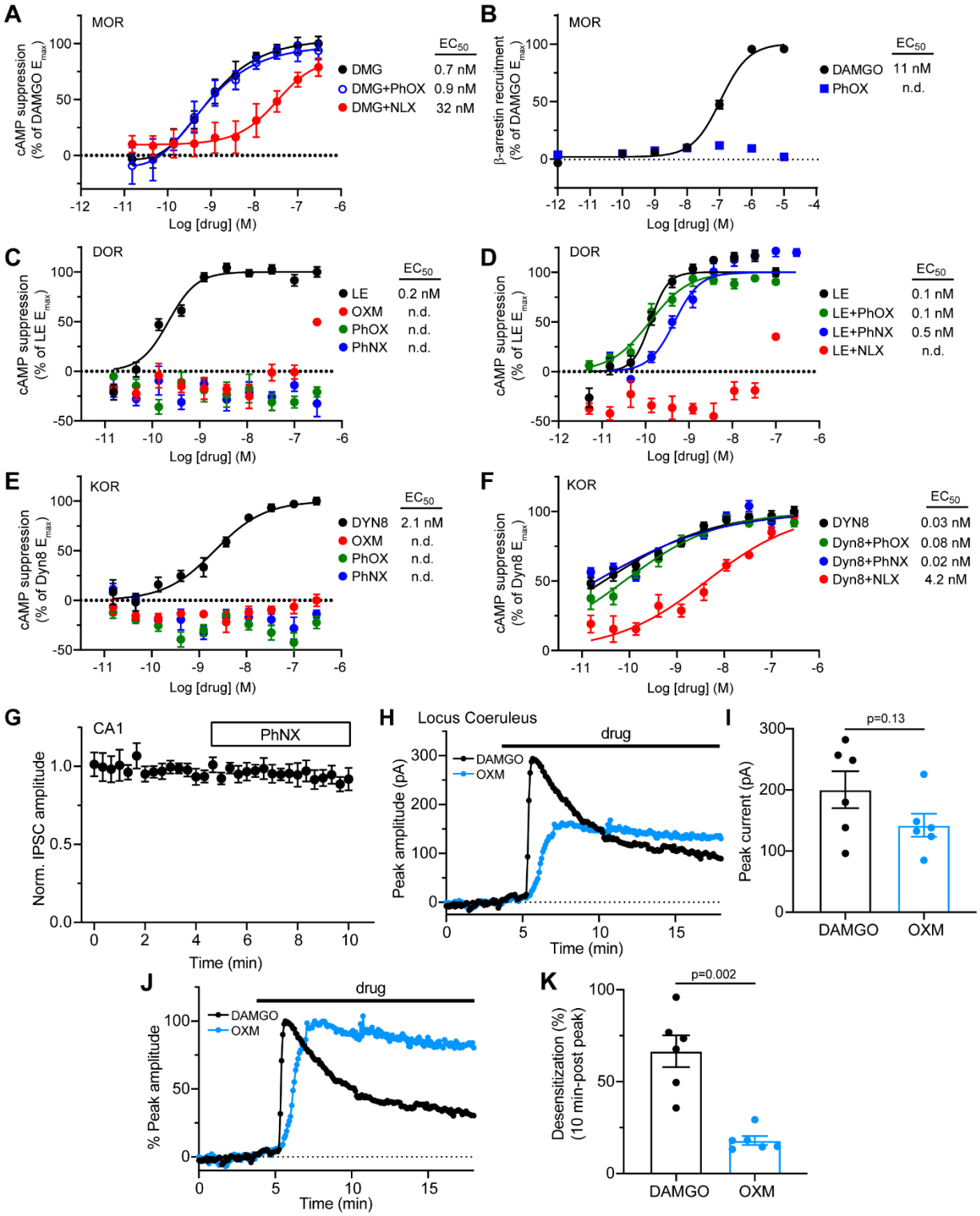

Figure S3. Further *in vitro* evaluation of PhOX and PhNX residual activity at mu, delta, and kappa opioid receptors *in vitro* and of PhOX in brain slices of rat LC, Related to Figures 1 and 2. (A) Agonist dose-response curves at the MOR for DAMGO

(DMG) in the absence and presence of NLX (100 nM) or PhOX (300 nM) using a cAMP assay. The solid line depicts the best-fit sigmoidal function used to derive the indicated EC_{50} value. Data were normalized to the response produced by DAMGO (1 μM) and are expressed as mean±SEM (n=5 wells per concentration). **(B)** Agonist dose-response curves at the MOR for DAMGO and PhOX using a NanoBiT-based luminescence complementation assay of β-arrestin signaling in HEK293T cells (n=4 wells per concentration). Data were normalized to the maximal response to DAMGO (10 μM) and are expressed as the mean ± SEM. **(C)** Agonist dose-response curves at the DOR for [Leu]^5-enkephalin (LE), OXM, PhOX, and PhNX, normalized to the response produced by LE (300 nM), presented as in A. **(D)** Agonist dose-response curves at the DOR for LE in the absence and presence of NLX (100 nM), PhOX (300 nM), or PhNX (300 nM) using a cAMP assay, presented as in A. **(E)** Agonist dose-response curves at the KOR for Dynorphin A(1-8) (Dyn8), OXM, PhOX, and PhNX, normalized to the response produced by Dyn8 (300 nM), presented as in A. **(F)** Agonist dose-response curves at the KOR for Dyn8 in the absence and presence of NLX (100 nM), PhOX (300 nM), or PhNX (300 nM), presented as in A. **(G)** Baseline-normalized inhibitory post-synaptic currents (IPSCs) in response to bath application of PhNX (1 μM) in hippocampus, at the time indicated by the black line (n=9 cells from 7 mice) (right). **(H)** Example currents evoked by bath application of DAMGO and oxymorphone (OXM) in whole-cell voltage clamp recordings from rat LC neurons. **(I)** Plot summarizing the peak currents produced by DAMGO and OXM (DAMGO: n=6 cells from 3 rats, OXM: n=6 cells from 3 rats, unpaired two-tailed t-test). **(J)** Same data as (B) but peak-normalized to emphasize the difference in desensitization. **(K)** Plot summarizing the % desensitization 10 minutes after the peak current was reached for the same cells shown in (C) (Mann-Whitney test). All data are plotted as mean ± SEM.

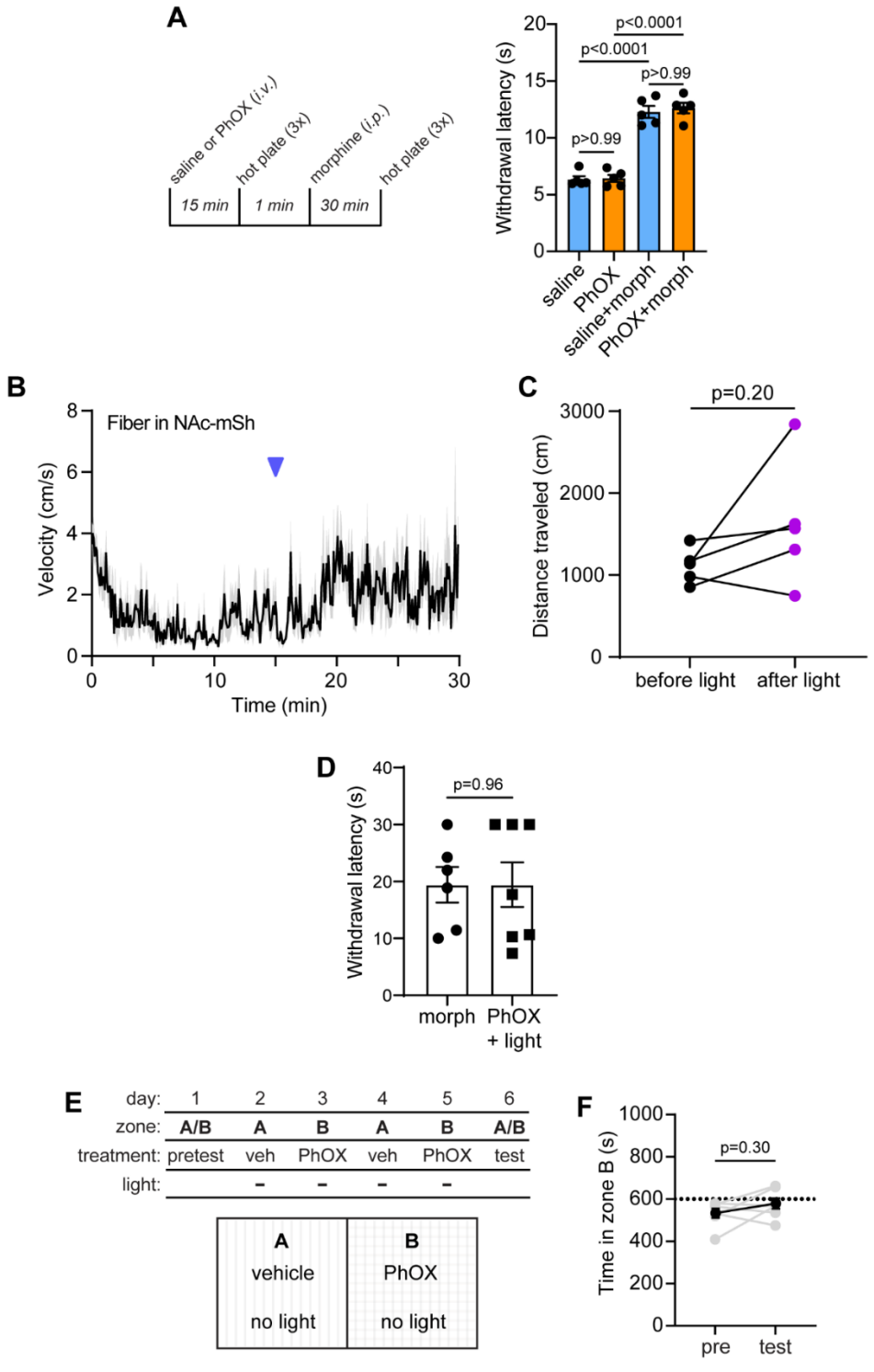

Figure S4, Related to Figure 4. PhOX does not produce analgesia or alter systemic morphine analgesia in the absence of illumination. (A) Experimental timeline (left) and

hot plate paw withdrawal latencies observed after injecting mice with either saline or PhOX (15 mg/kg *i.v.*), followed by morphine (5 mg/kg, *s.c.*) (n=5 mice, One-way ANOVA, $F(3,16)=73.21$, $p<0.0001$, Bonferroni's multiple comparisons test) (right). **(B)** Plot of average velocity over time (n=5 mice) before and after PhOX photoactivation in the NAc-mSh. **(C)** Summary plot comparing the distance traveled in the 15 minutes before and after PhOX photoactivation (paired two-tailed t-test). **(D)** Plot comparing the tail-flick withdrawal latencies 30 minutes after morphine (10 mg/kg) administration or 1 minute after unilateral PhOX uncaging in the PAG (Mann-Whitney test). **(E)** Schematic indicating condition place preference (CPP) context-stimuli pairings for PhOX administration without uncaging. **(F)** Time spent in zone B on test days (n=7 mice, Wilcoxon test). All data are plotted as mean ± SEM.

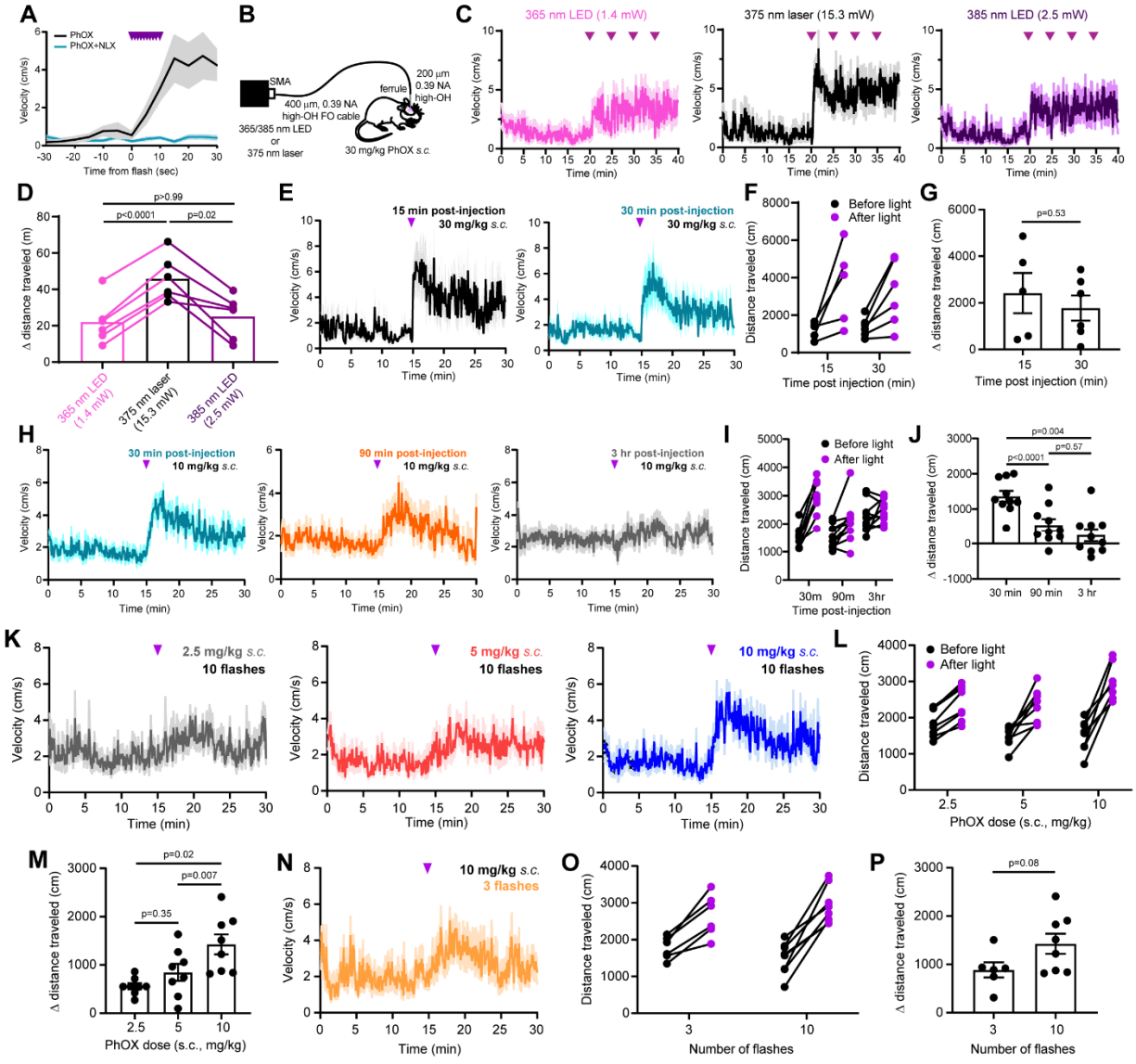

Figure S5. Rapid locomotor activation and comparison of locomotor responses evoked by PhOX photoactivation under various conditions, Related to Figure 5. (A) Data presented in Figure 5B zoomed in around the train of 375 nm light flashes. Data are plotted as mean ± SEM. **(B)** Schematic indicating the direct coupling of light from either a 365 nm LED, a 385 nm LED, or a 375 nm laser into an optical fiber implanted over the VTA. The 400 µm, 0.39 NA high-OH coupling fiber was found to maximize the transfer of LED output to the output of a ferrule-coupled 200 µm, 0.39 NA optical fiber similar to those implanted in the mice. Maximal output from the 365 nm LED was 1.4 mW and 2.5 mW from the 385 nm LED. The 375

nm laser output was set to 15.3 mW in order to evoke a relatively strong locomotor response. **(C)** Average plots of velocity over time in the open field using trains of 10 x 200 ms flashes of light (1 Hz) at the times indicated by each arrow, using the indicated light sources (n=6 mice per condition). **(D)** Summary plot of the change in total distance traveled in the 20 minutes before and after light delivery (n=6 mice, Repeated measures one-way ANOVA, F(1.12,5.62)=20.99, p=0.004, Bonferroni's multiple comparisons test). Neither LED at maximal power was as effective as 15.3 mW from the 375 nm laser, but both LEDs evoked similar locomotor responses. **(E)** Average plots of velocity over time in the open field before in response to 375 nm light (10 x 200 ms, 1 Hz, 70 mW) either 15 min or 30 min after PhOX (30 mg/kg, *i.v.*) administration (15 min: n = 5 mice, 30 min: n=6 mice). **(F)** Plot of the total distance traveled in the 15 minutes before and after photoactivation. **(G)** Summary plot of the change in total distance traveled in the 15 minutes before and after light delivery (Unpaired two-tailed t-test, 15 min: n=5 mice, 30 min: n=6 mice). **(H)** Average plots of velocity over time in the open field in response to 375 nm light (10 x 200 ms, 1 Hz, 20 mW) either 30 min, 90 min, or 3 hr after PhOX (10 mg/kg, *s.c.*) administration (n=10 mice). **(I)** Same as (B) but for the data in (D). **(J)** Same as (C) but for the data in (D) (Repeated measures one-way ANOVA, n=10 mice, F(1.2, 11.0)=13.1, p=0.0029, Tukey's multiple comparisons test). **(K)** Average plots of velocity over time in the open field using 10 x 200 ms flashes of 375 nm light (2 Hz, 70 mW) at the indicated doses of PhOX (n = 8 mice). **(L)** Plot of the total distance traveled in the 15 minutes before and after photoactivation. **(M)** Summary plot of the change in total distance traveled in the 15 minutes before and after light delivery (n=8 mice, Repeated measures one-way ANOVA, F(1.41,8.84)=10.32, p=0.006, Tukey's multiple comparisons test). **(N)** Average plots of velocity over time in the open field using 3 x 200 ms flashes of 375 nm light (2 Hz, 70 mW) at 10 mg/kg PhOX (n = 6 mice). **(O)** Plot of the total distance traveled in the 15 minutes before and after photoactivation (10 flash data are the same as in A-C). **(P)** Summary plot of the change in total distance traveled in the 15 minutes before and after light delivery (Unpaired two-tailed t test, 3 flashes: n=6 mice, 10 flashes: n=8 mice). Although 10 flashes produced a larger average locomotor response than 3 flashes, the difference was not statistically significant. All data are plotted as mean ± SEM.

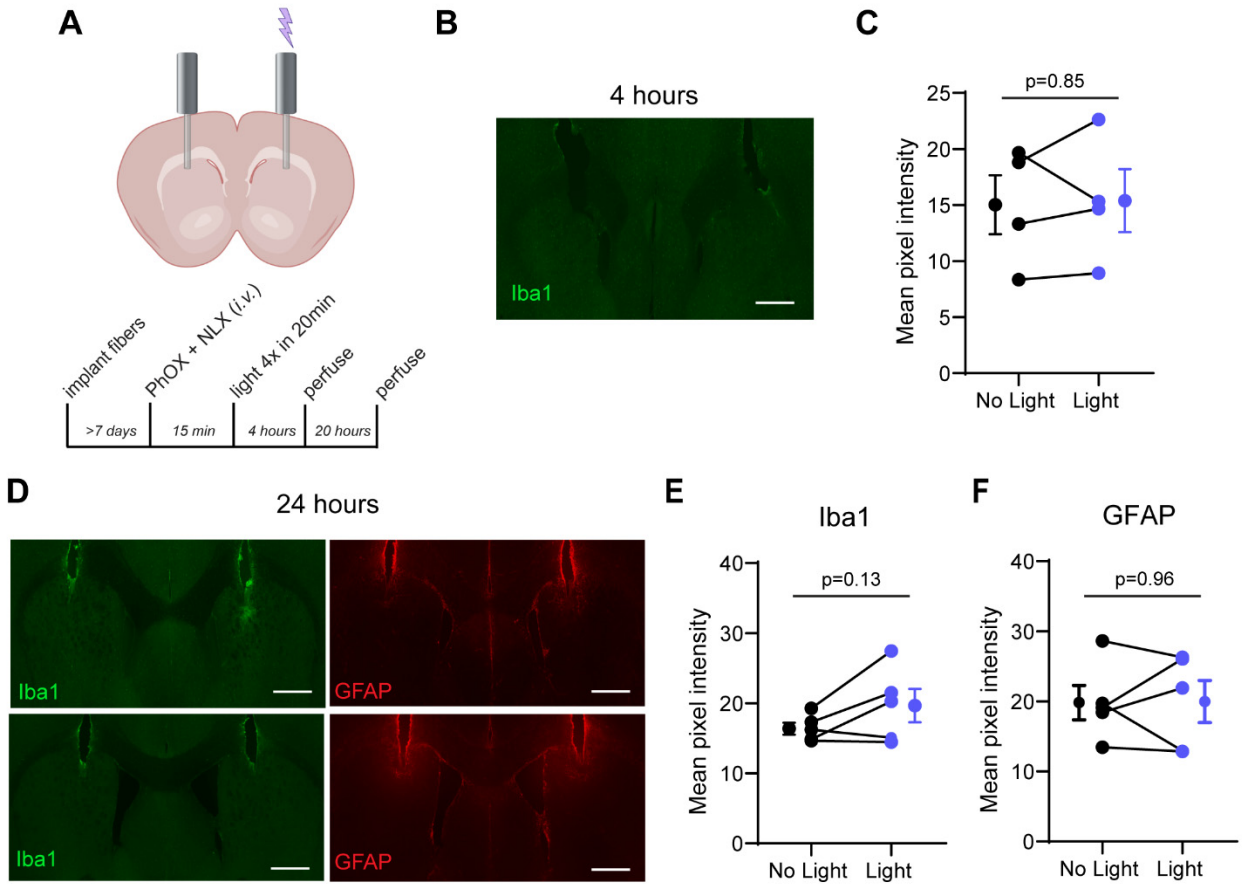

Figure S6. Expression of microglia and astrocyte markers after PhOX photoactivation in the presence of NLX in the dorsal striatum, Related to Figure 5. **(A)** Schematic indicating the bilateral implantation optical fibers in the dorsal striatum, with only one hemisphere connected to the 375 nm laser such that the other serves as a negative control (top), and experimental timeline (bottom). **(B)** Representative immunofluorescence image of Iba1 expression at the site of fiber implantation in brains harvested 4 hr after PhOX uncaging (scale bar=1 mm). **(C)** Mean pixel intensity of Iba1 immunofluorescence in the hemisphere of photoactivation compared to the contralateral hemisphere in brains harvested 4 hr after photoactivation (n=4 mice, paired two-tailed t-test). **(D)** Representative immunofluorescence images of Iba1 and GFAP expression in brains harvested 24 hr after PhOX uncaging (scale bar=1 mm). Whereas the top image series shows some Iba1 signal under the illuminated fiber, this was only observed in 3/5 mice; the bottom image series is from a mouse that did not exhibt Iba1 signal. **(E)** Mean pixel intensity of Iba1 immunofluorescence in the hemisphere of photoactivation compared to the contralateral hemisphere in brains harvested 24 hr after photoactivation (n=5 mice, paired two-tailed t-test). **(F)** Same as (E) but for GFAP (n=5 mice, paired two-tailed t-test). All data are plotted as mean ± SEM.

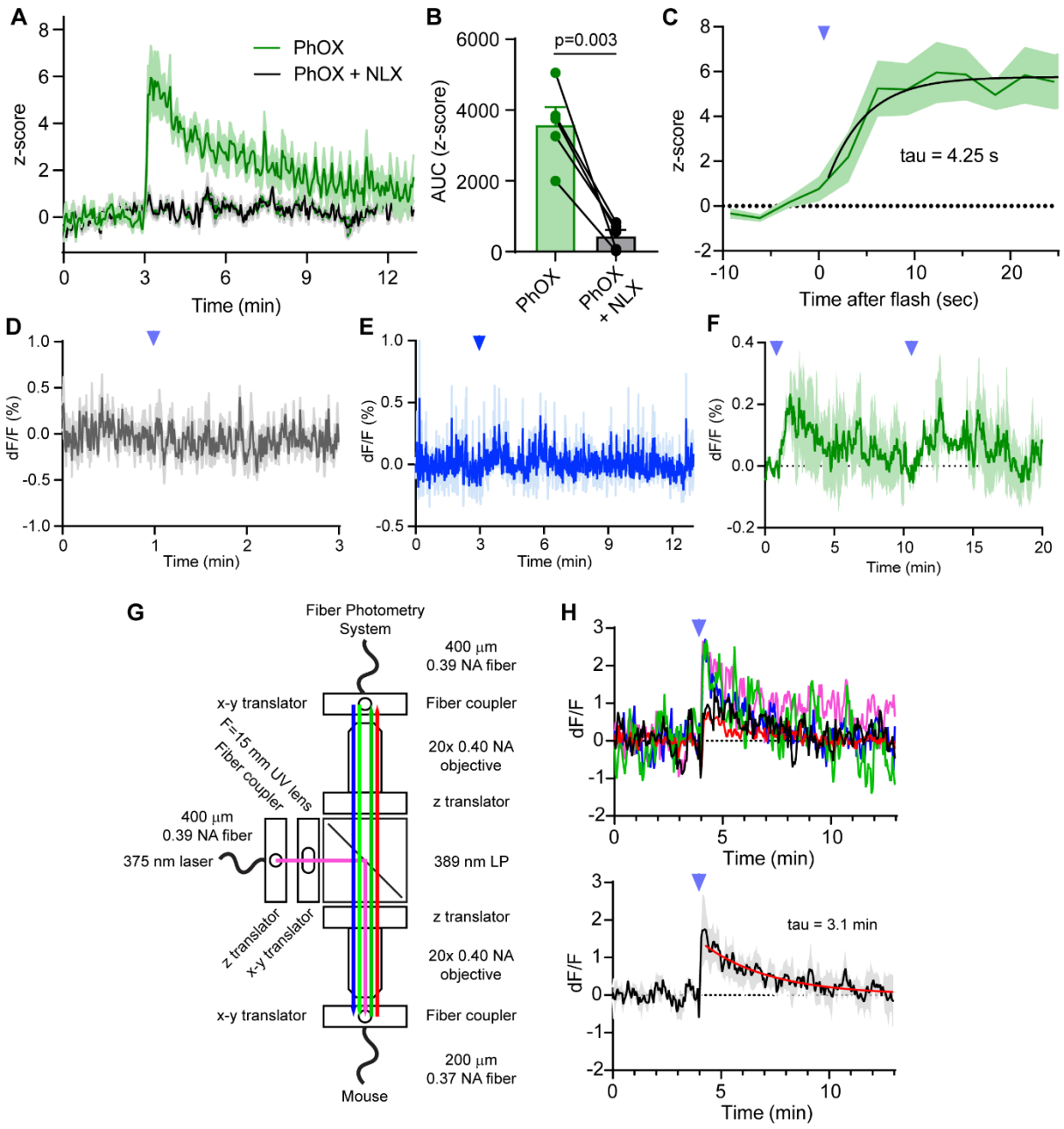

Figure S7. Further characterization of NAc-mSh dopamine release evoked by PhOX photoactivation in the VTA and details of the optical relay used combining UV uncaging with fiber photometry, Related to Figure 6. (A) Average dLight1.3b fluorescence (z-score) in the NAc-mSh in response to PhOX uncaging with a single 375 nm light flash in the ipsilateral VTA (200 ms, 50 mW) after systemic injection of either PhOX (15 mg/kg *i.v.*) or PhOX + NLX (15 mg/kg & 10 mg/kg, *i.v.*, n=5 mice). Same data shown in Figure 6C (n=5 mice). **(B)** Summary plot of the uncaging-evoked dlight1.3b fluorescence changes (z-score) shown in (A) (AUC=area under the curve, n=5 mice, paired Student's t-test). **(C)** Zoom-in of the

rising phase of the dLight1.3b signal shown in Supporting Figure 10A (n=5 mice). **(D)** Average dLight1.3b fluorescence in the NAc-mSh in response to a single 375 nm light flash in the ipsilateral VTA (200 ms, 50 mW) in the absence of PhOX (n=4 mice). **(E)** Average dLight1.3b fluorescence in the NAc-mSh in response to 473 nm light flashes (10 x 200 ms, 50 mW, 1 Hz) in the ipsilateral VTA (200 ms, 50 mW) after systemic injection of PhOX (15 mg/kg *i.v.*) (n=2 mice). **(F)** Average dLight1.3b fluorescence in the NAc-mSh in response to repeated PhOX uncaging with two single 375 nm light flashes in the ipsilateral VTA (200 ms, 20 mW) after systemic injection of PhOX (10 mg/kg *s.c.*) (n=3 mice). **(G)** Schematic depicting the fiber photometry relay system used to integrate 375 nm laser light into the fiber photometry output pathway. **(H)** Fluorescence artifact produced by UV excitation of jGCaMP8s with a single light flash in the absence of PhOX (200 ms, 20 mW). Average fluorescence responses to 3 UV flashes, applied every 10 min, in individual mice (top) and average fluorescence response of all mice combined (bottom, single exponential least-squares curve fit, n=5 mice). The average artifacts from individual mice (top) were removed from the data obtained in the presence of PhOX to generate the artifact-corrected data shown in Figure 6K. All data are plotted as mean ± SEM.

Data S1: 1H NMR spectra, 13C NMR spectra, and HRMS spectra, related to Figure 1.

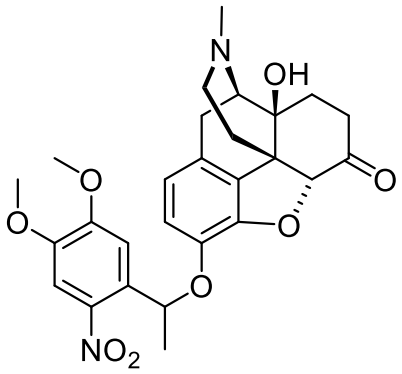

PhOX

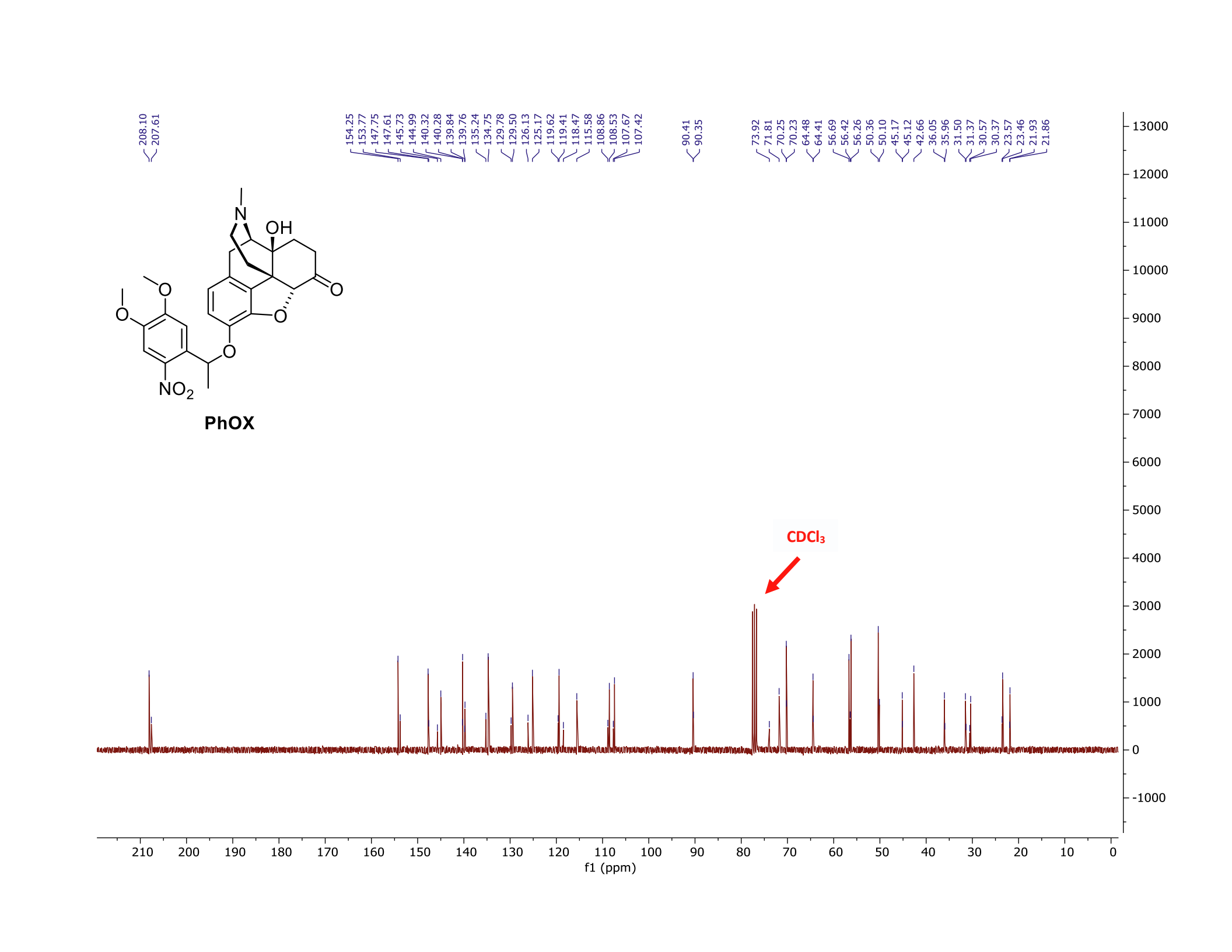
208.10
207.61
154.25
153.77
147.75
147.61
145.73
144.99
140.32
140.28
139.84
139.76
135.24
134.75
129.78
129.50
126.13
125.17
119.62
119.41
118.47
115.58
108.86
108.53
107.67
107.42
90.41
90.35
73.92
71.81
70.25
70.23
64.48
64.41
56.69
56.42
56.26
50.36
50.10
45.17
45.12
42.66
36.05
35.96
31.50
31.37
30.57
30.37
23.57
23.46
21.93
21.86
N
OH
O
O
O
O
O
NO2
PhOX
CDCl3
13000
12000
11000
10000
9000
8000
7000
6000
5000
4000
3000
2000
1000
0
-1000
210
200
190
180
170
160
150
140
130
120
110
100
90
80
70
60
50
40
30
20
10
0
f1 (ppm)

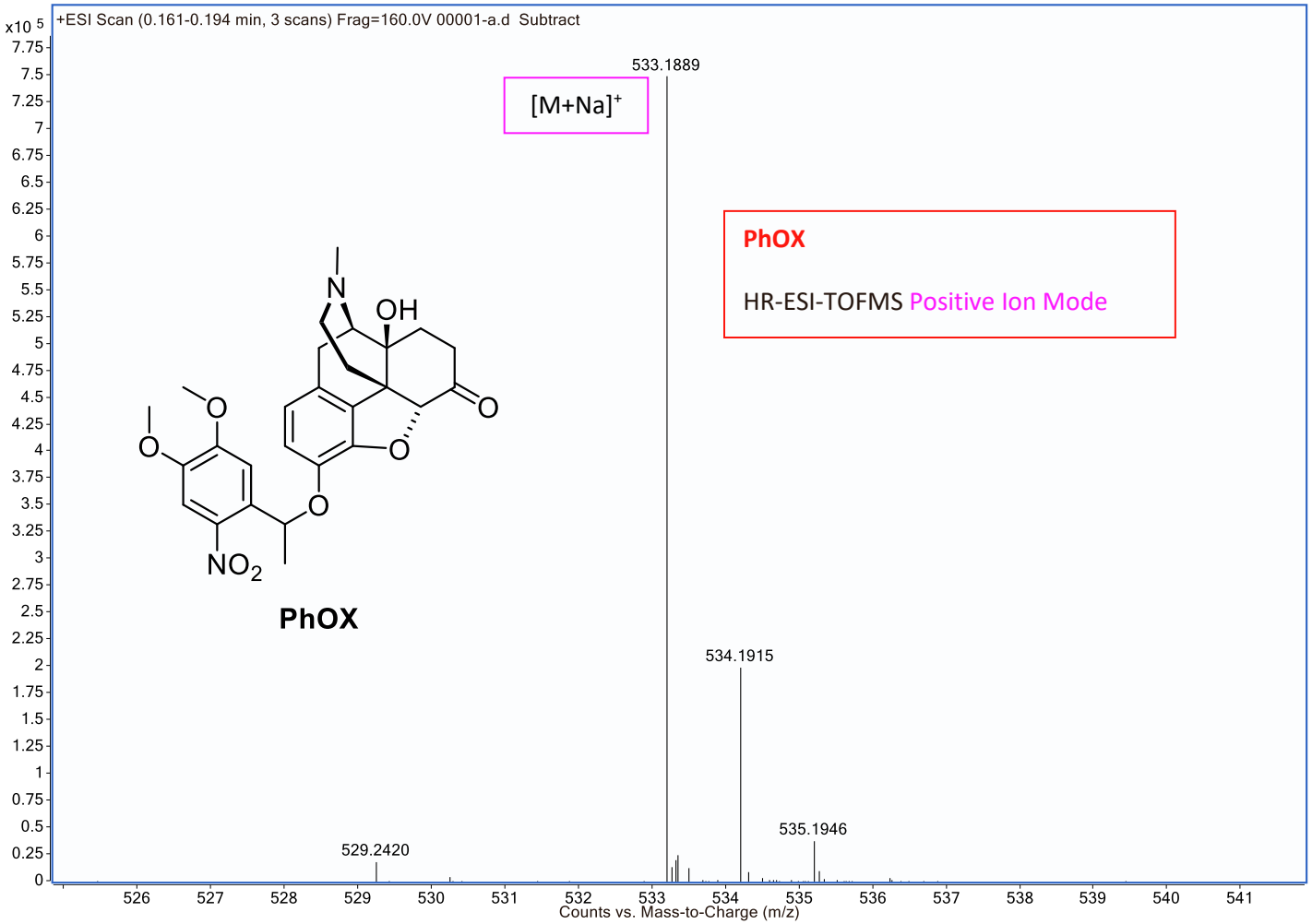

PhOX

Search Results: PhOX

Mass Measured	Theo. Mass	Delta (ppm)	Composition
533.1889	533.1894	-0.9	$[C_{27}H_{30}N_2O_8Na]^+$

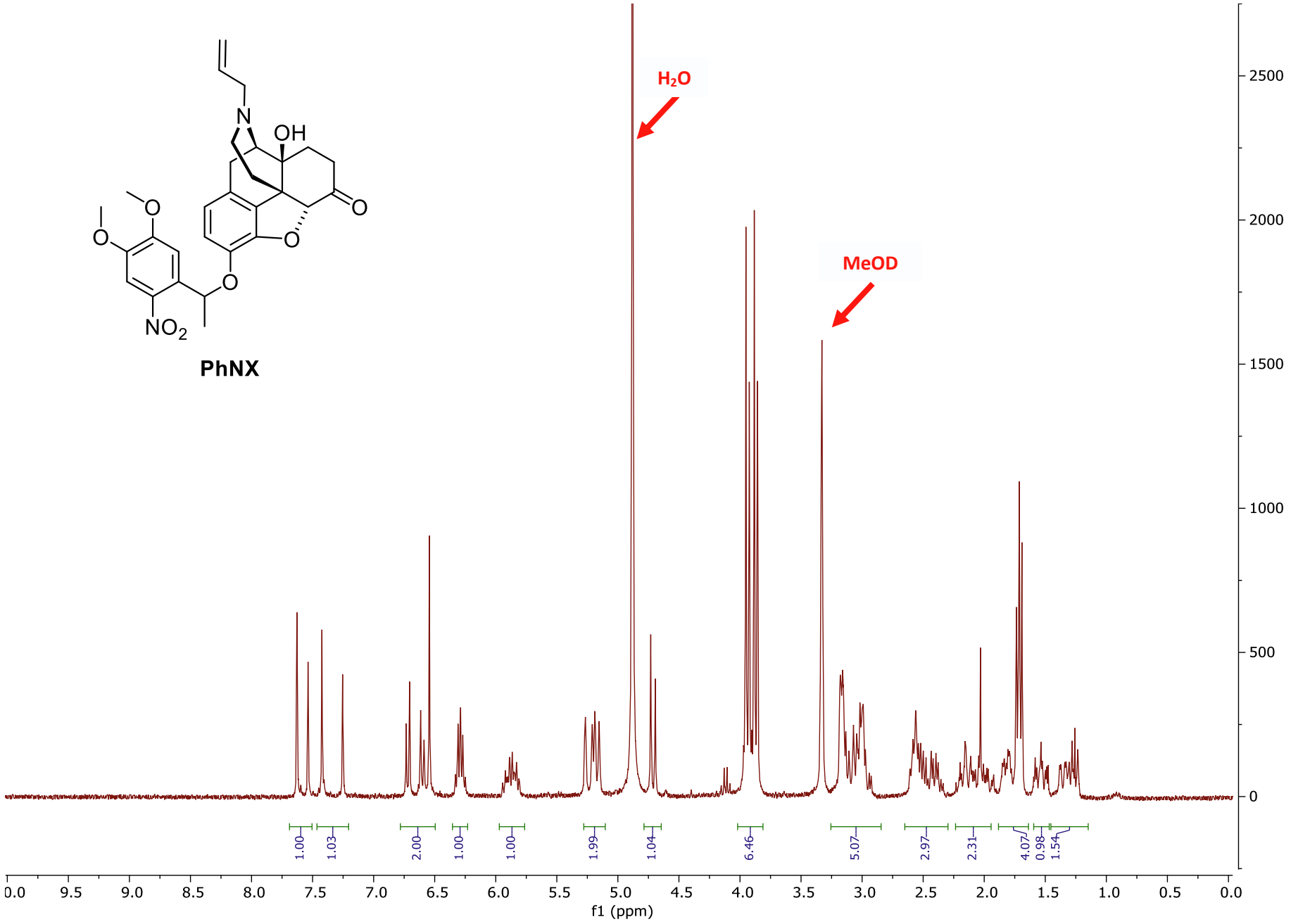
H2O
MeOD
PhNX
f1 (ppm)

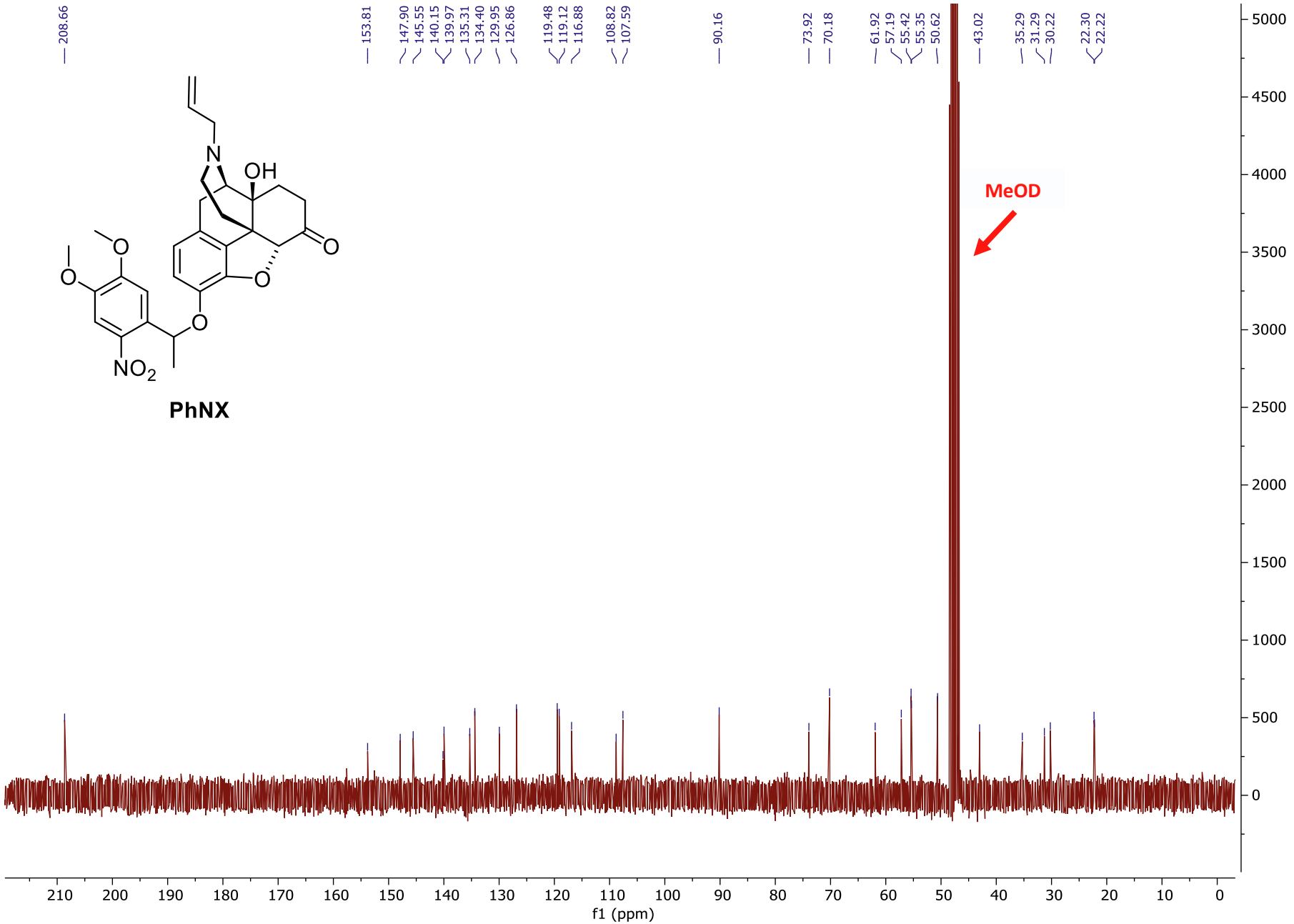
208.66
153.81
147.90
145.55
140.15
139.97
135.31
134.40
129.95
126.86
119.48
119.12
116.88
108.82
107.59
90.16
73.92
70.18
61.92
57.19
55.42
55.35
50.62
43.02
35.29
31.29
30.22
22.30
22.22
MeOD
PhNX
f1 (ppm)

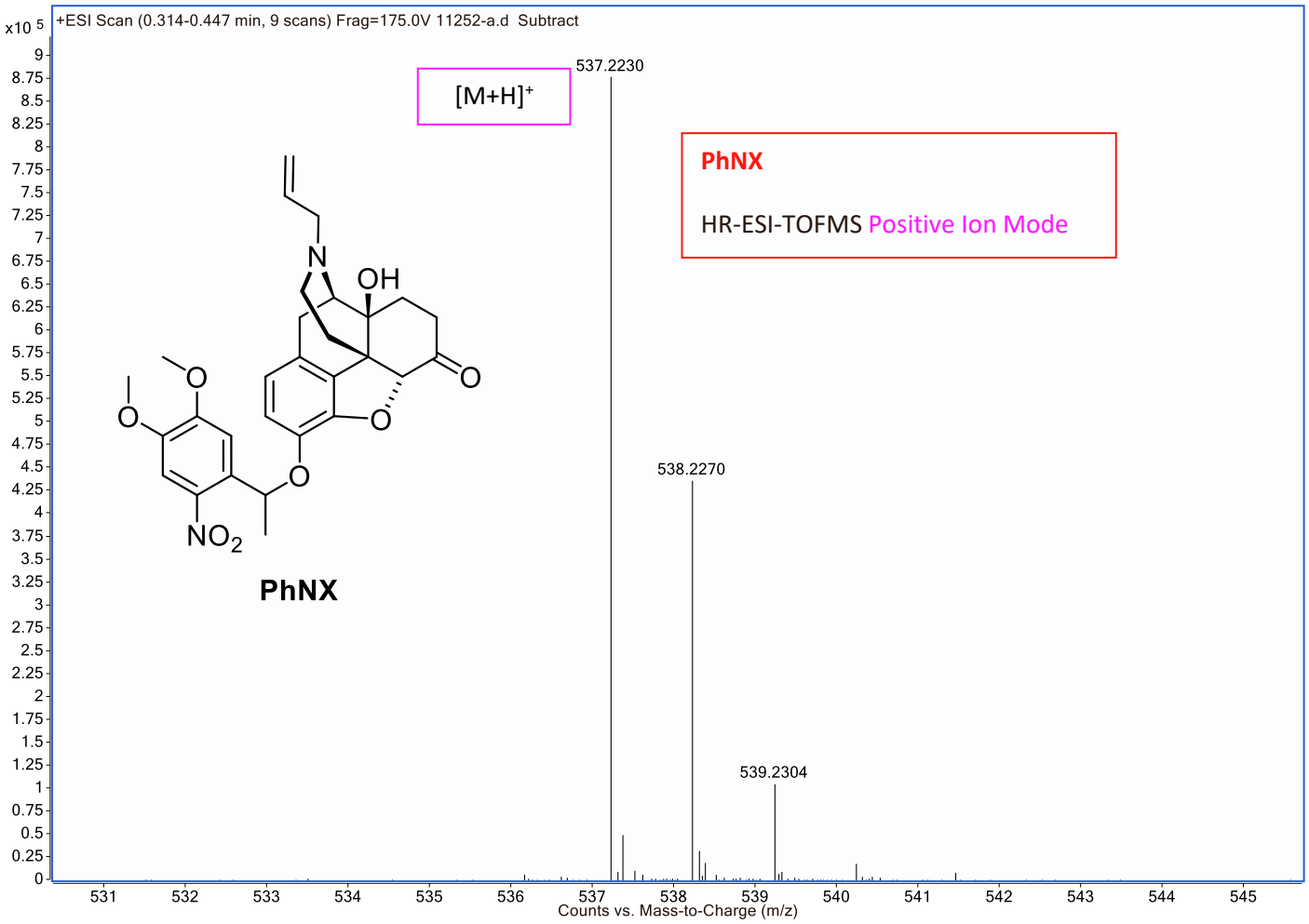

Search Results: PhNX

Mass Measured	Theo. Mass	Delta (ppm)	Composition
537.2230	537.2231	-0.5	$[C_{29}H_{33}N_2O_8]^+$

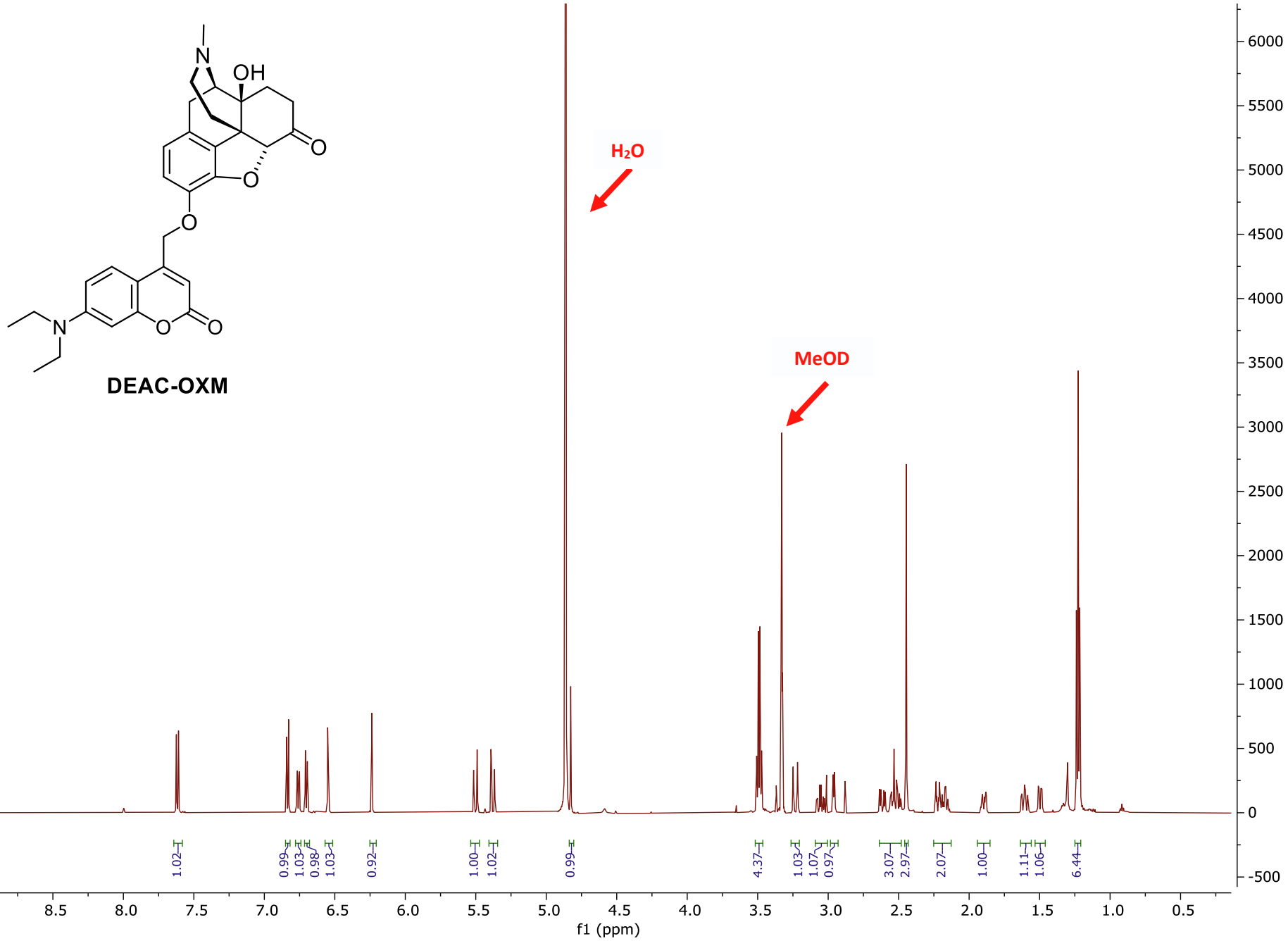
DEAC-OXM
H₂O
MeOD
f1 (ppm)

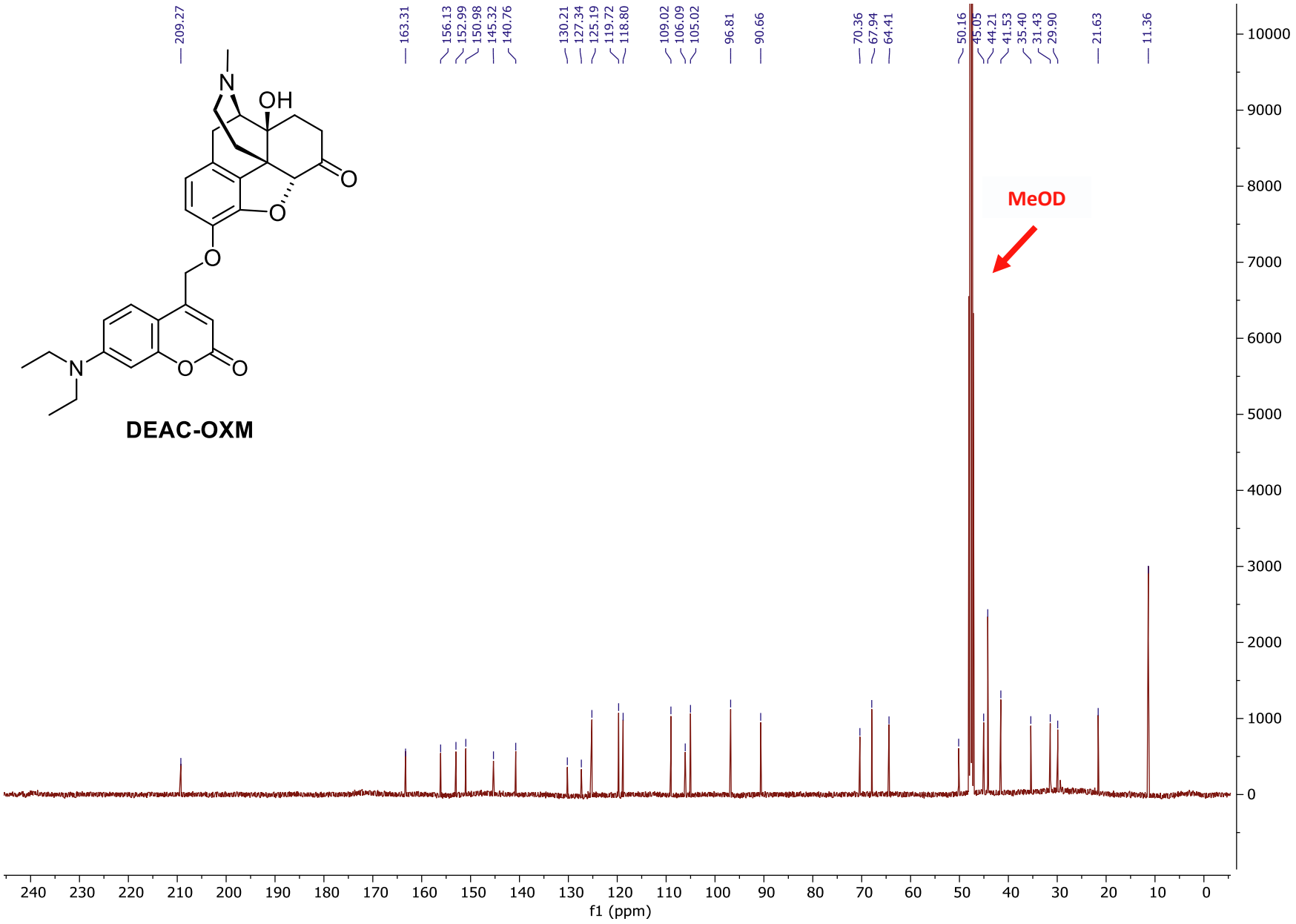
209.27
163.31
156.13
152.99
150.98
145.32
140.76
130.21
127.34
125.19
119.72
118.80
109.02
106.09
105.02
96.81
90.66
70.36
67.94
64.41
50.16
45.05
44.21
41.53
35.40
31.43
29.90
21.63
11.36
MeOD
DEAC-OXM
f1 (ppm)

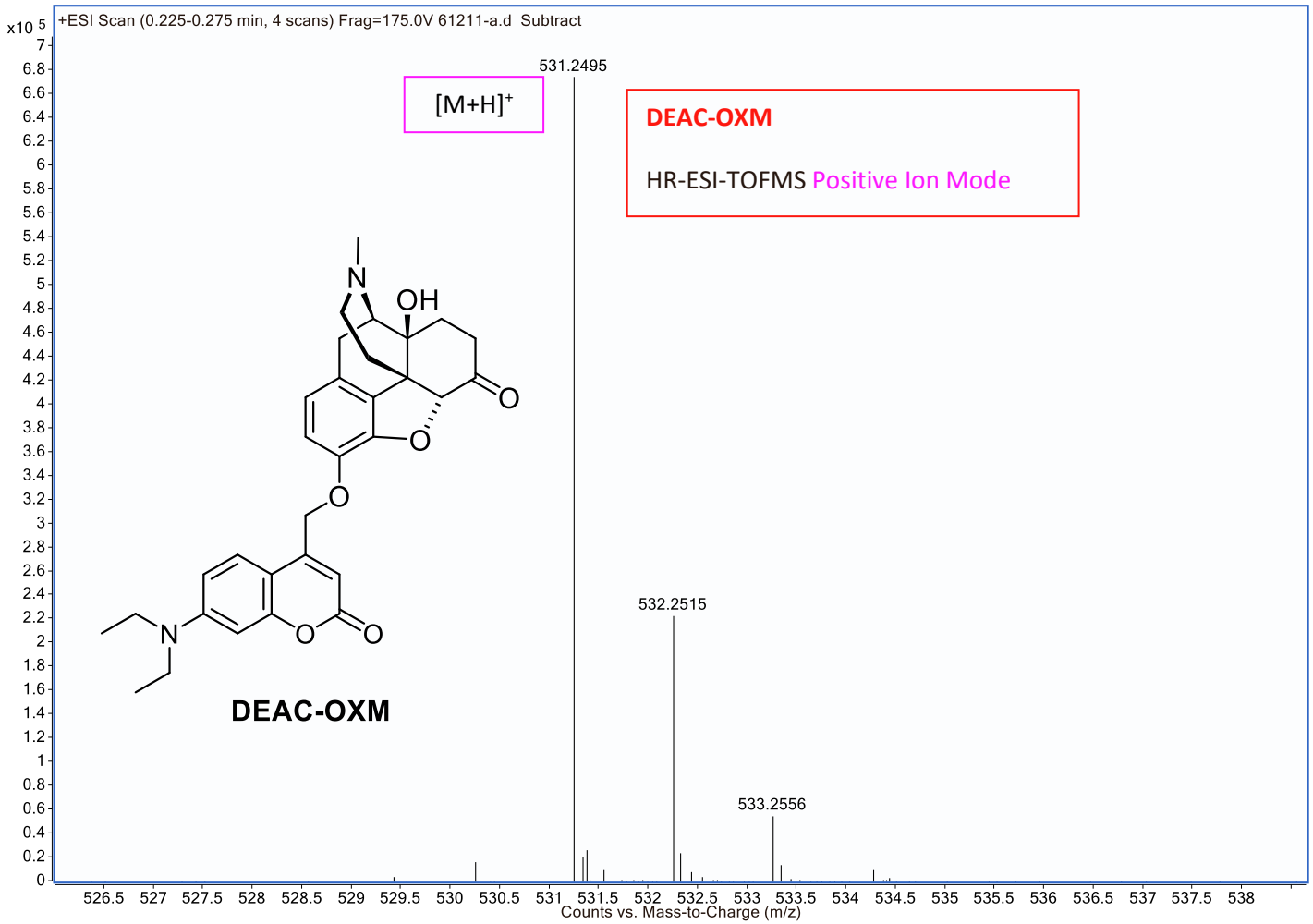

Search Results: DEAC-OXM

Mass Measured	Theo. Mass	Delta (ppm)	Composition
531.2495	531.2490	0.9	$[C_{31}H_{35}N_2O_6]^+$

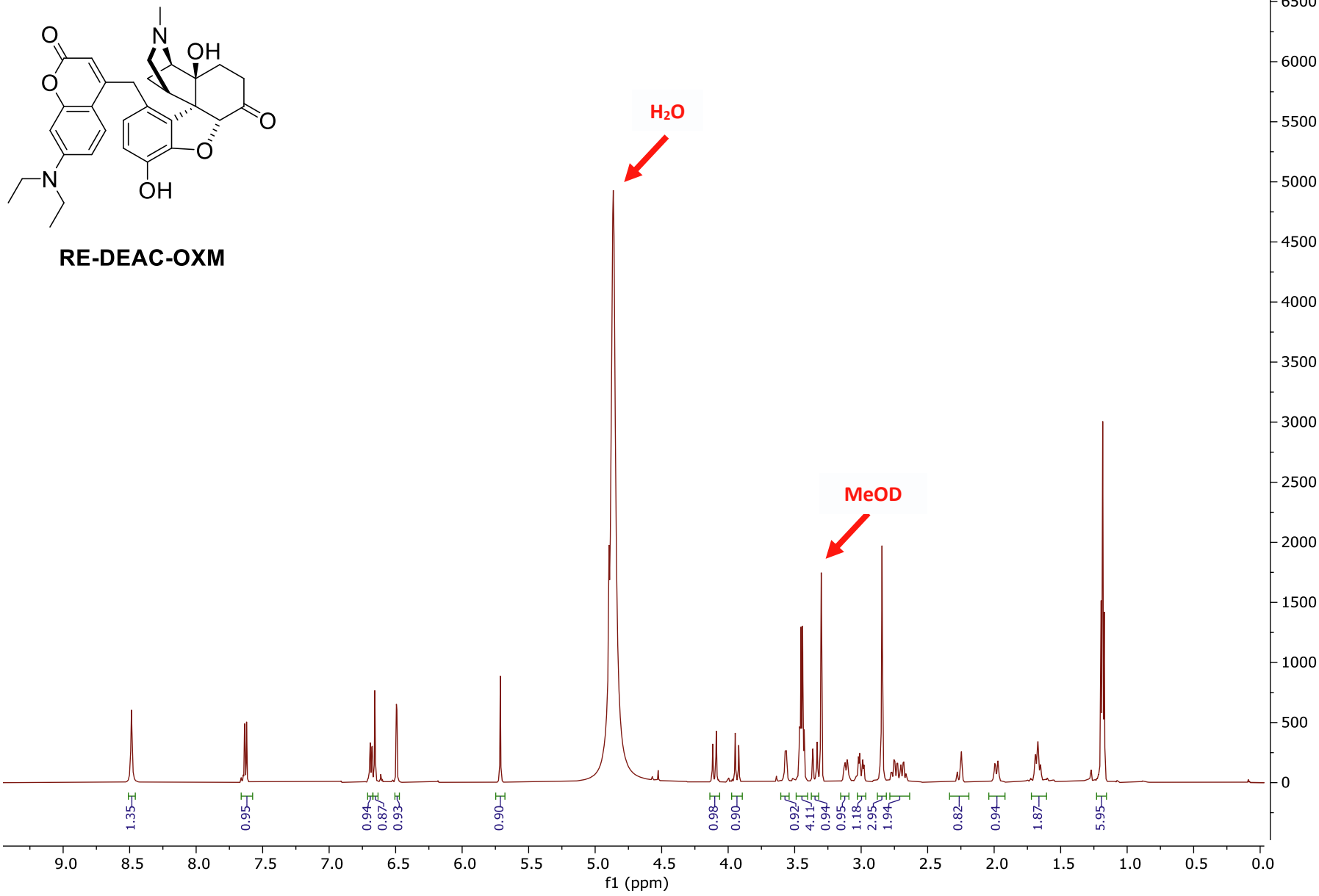
RE-DEAC-OXM
H2O
MeOD
f1 (ppm)

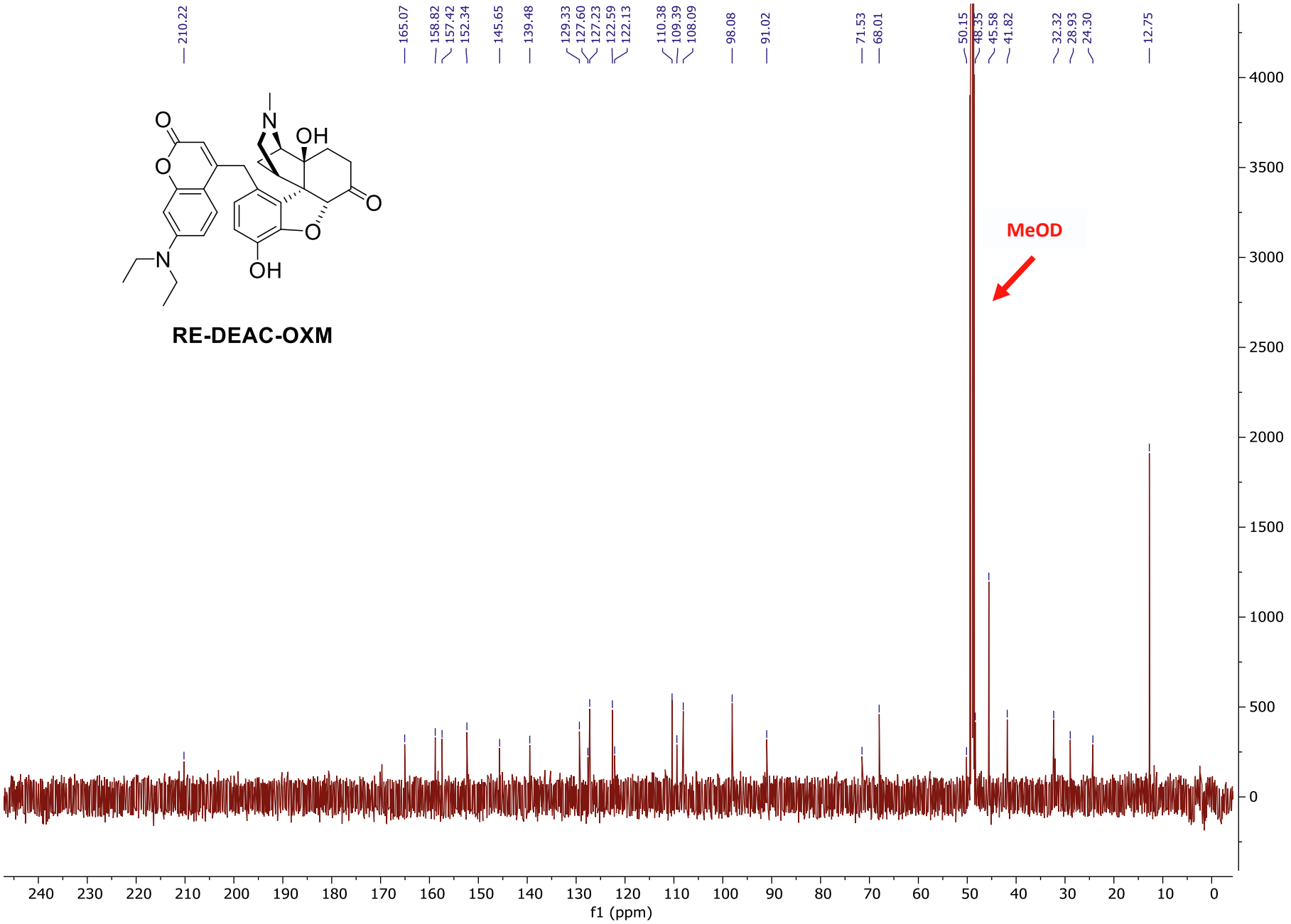
210.22
165.07
158.82
157.42
152.34
145.65
139.48
129.33
127.60
127.23
122.59
122.13
110.38
109.39
108.09
98.08
91.02
71.53
68.01
50.15
48.35
45.58
41.82
32.32
28.93
24.30
12.75
MeOD
RE-DEAC-OXM
f1 (ppm)

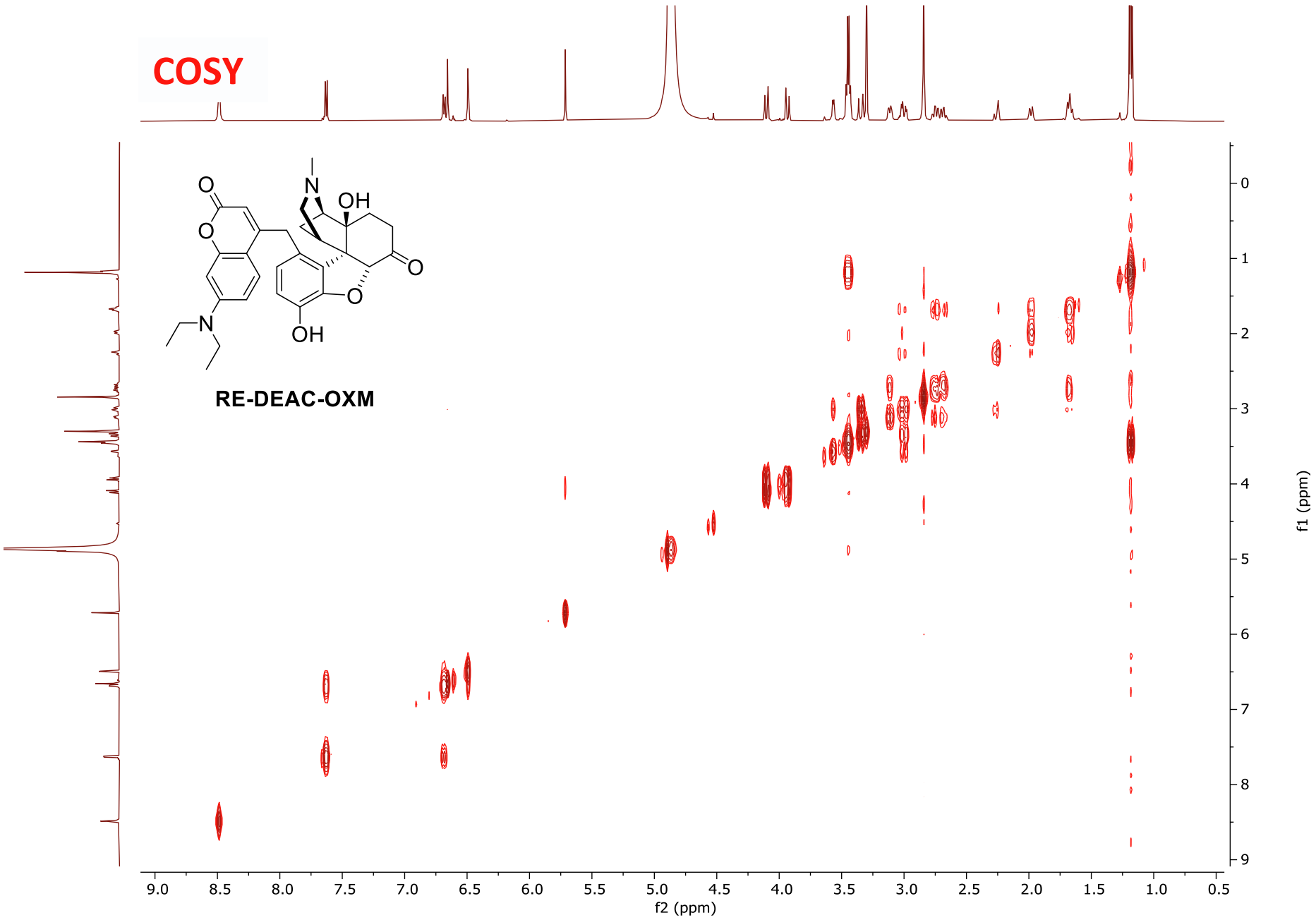
COSY
RE-DEAC-OXM
f2 (ppm)
f1 (ppm)

HSQC

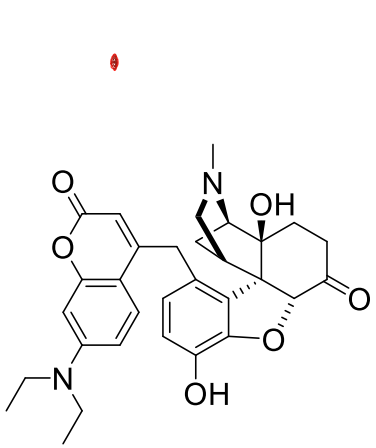

RE-DEAC-OXM

f2 (ppm)

f1 (ppm)

NOESY

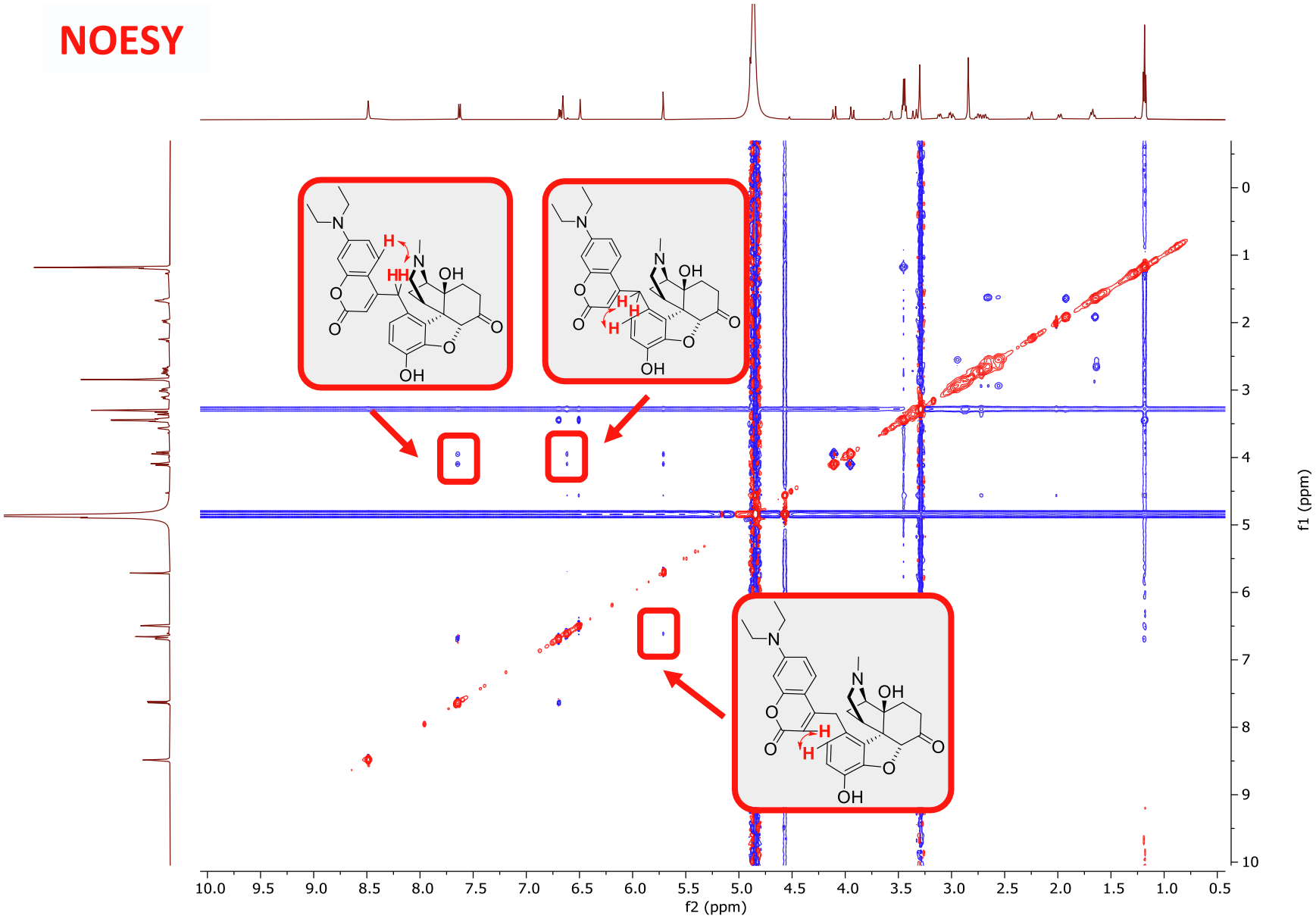
f2 (ppm)
f1 (ppm)
10.0
9.5
9.0
8.5
8.0
7.5
7.0
6.5
6.0
5.5
5.0
4.5
4.0
3.5
3.0
2.5
2.0
1.5
1.0
0.5
0
1
2
3
4
5
6
7
8
9
10
OH
O
N
H
HH

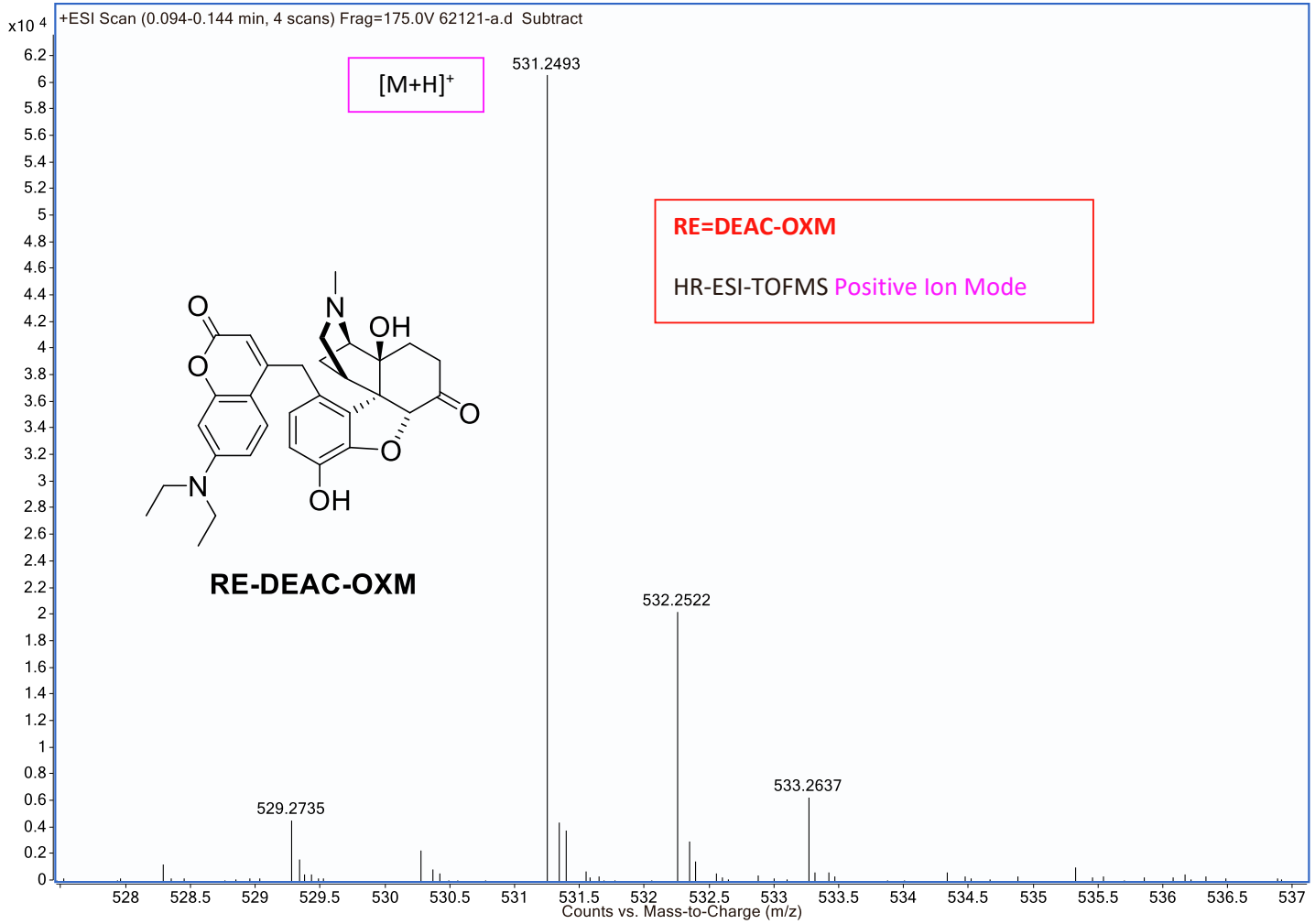

Search Results: RE-DEAC-OXM

Mass Measured	Theo. Mass	Delta (ppm)	Composition
531.2493	531.2490	0.6	$[C_{31}H_{35}N_2O_6]^+$

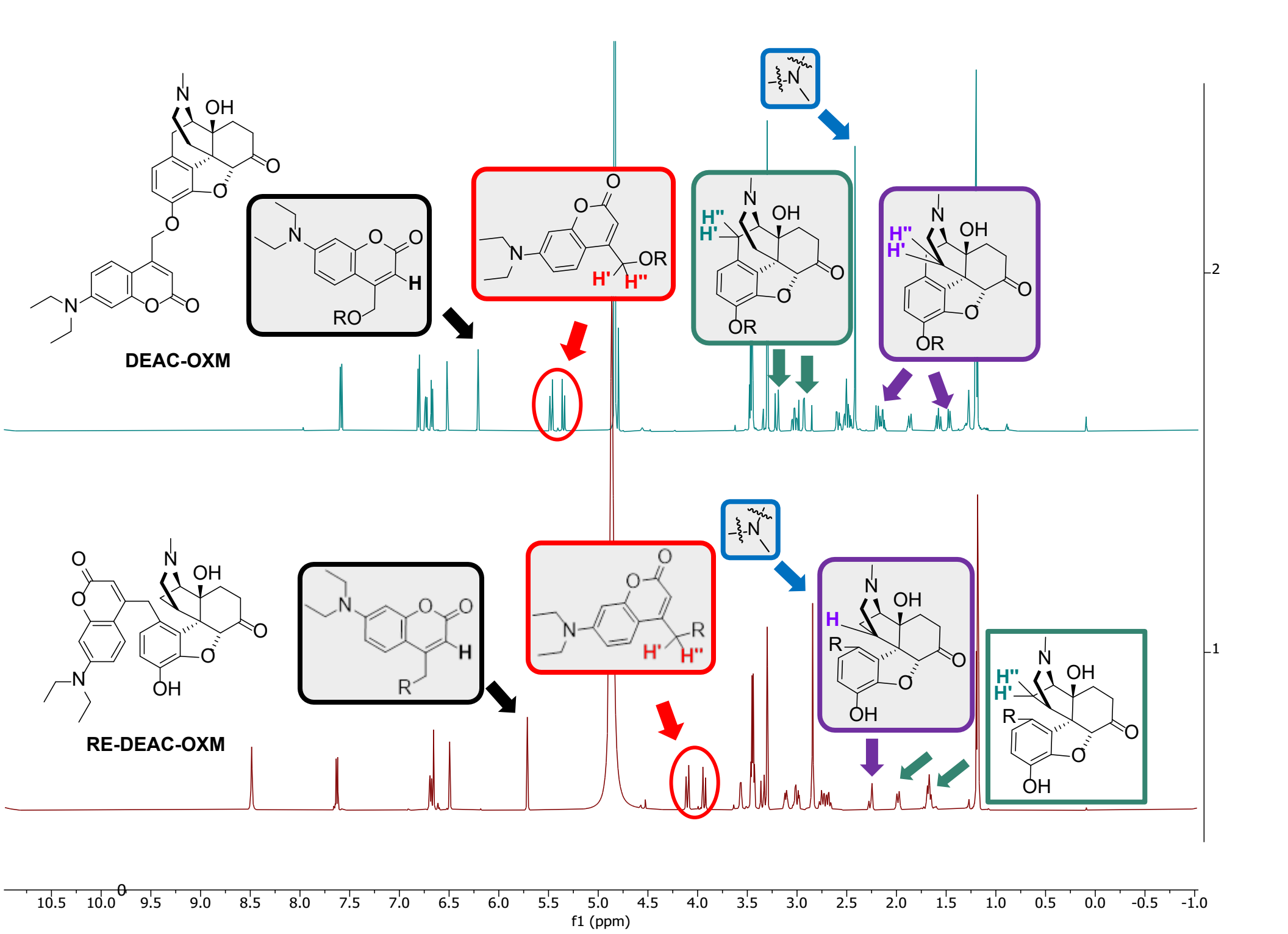
DEAC-OXM
RE-DEAC-OXM
H'
H''
H
R
OR
OH
2
1
0
10.5 10.0 9.5 9.0 8.5 8.0 7.5 7.0 6.5 6.0 5.5 5.0 4.5 4.0 3.5 3.0 2.5 2.0 1.5 1.0 0.5 0.0 -0.5 -1.0
f1 (ppm)